Journal of Biomolecular NMR **30:** 133–142, 2004.

Measurement of ^{15}N csa/dipolar cross-correlation rates by means of Spin State Selective experiments

Sabine Bouguet-Bonnet, Pierre Mutzenhardt* & Daniel Canet
Laboratoire de Méthodologie RMN, Université Henri Poincaré, Faculté des Sciences, BP 239, 54506 Vandoeuvre-lès-Nancy Cedex, France

Received 2 March 2004; Accepted 19 June 2004

Key words: cross-correlation, multidimensional NMR, NMR, relaxation, spin-state-selective excitation

Abstract

We propose a method for the determination of ^{15}N csa/dipolar cross-correlation rates based on the measurement of the two apparent transverse (or longitudinal) relaxation rates associated with each component of the nitrogen doublet (N^{α} and N^{β}). This is achieved by inserting a spin state selective scheme in conventional inverse Carr-Purcell-Meiboom-Gill (or inversion-recovery) pulse sequence which allows for the edition of a HSQC-type spectrum for each of the spin states. Transverse cross-correlation rates necessitate two independent sets of measurements (for N^{α} and N^{β}, respectively), whereas for longitudinal cross correlation rates, besides N^{α} and N^{β} measurements, the method requires the knowledge of both the ^{15}N longitudinal auto-relaxation rate and the longitudinal two-spin order ($2N_zH_z$) auto-relaxation rate. These additional parameters are mandatory because of the non-exponential behavior of the N^{α} and N^{β} longitudinal decays. Conversely, the present method does not require any complex manipulation of 2D spectra, the cross-correlation rates being obtained from the difference of the two (N^{α} and N^{β}) apparent relaxation rates. This approach is applied to ^{15}N-labelled ubiquitin at two different magnetic fields (9.4T and 14.1T).

Introduction

Cross-correlation between ^{1}H-^{15}N dipolar interaction and ^{15}N chemical shift anisotropy (csa) has proved to be of considerable interest due to the nature of the information they contain (Kumar et al., 2000; Brutscher, 2000; Frueh, 2002). This relaxation interference causes the two lines of a scalar-coupled *IS* spin system to have different line widths (Goldman, 1984) due to their different relaxation behavior. Such an effect has been successfully applied in the field of biological molecular studies; it is, in particular, the basis of the TROSY experiment (Pervushin et al., 1997), which selects the sharpest line of the ^{15}N doublet, thus making feasible NMR investigations of larger proteins. It is also used quantitatively to characterize the ^{15}N csa tensor (magnitude and orientation) (Tjandra et al., 1996; Fushman et al., 1998; Scheurer et al., 1999; Kover and Batta, 2001), and conformational exchange (Kroenke et al, 1998; Boisbouvier et al., 1999). Additionally, along with the classical relaxation rates (^{15}N longitudinal relaxation rate, R_1, ^{15}N transverse relaxation rate, R_2, and ^{1}H-^{15}N cross-relaxation rate, σ), cross-correlation rates appear quite complementary in order to define more accurately protein motion (Tjandra et al., 1996; Fushman et al., 1998; Boisbouvier et al., 1999).

Several approaches have been employed to access the csa/dipolar interference term in proteins and they could be classified in three main categories: (i) direct methods based on the ratio of in-phase and antiphase components of the ^{15}N (or ^{13}C) magnetization registered in two separate experiments (Tjandra et al., 1996; Tessari et al., 1997; Ghose et al., 1998), (ii) direct methods based on the different evolution of the doublet components (Kover and Batta, 2001; Boisbouvier et al., 1999; Hall et al., 2003a, b; Ferrage

*To whom correspondence should be addressed. E-mail: Pierre.Mutzenhardt@ rmn.uhp-nancy.fr

et al., 2004), (iii) indirect methods which yield cross-correlation rates from an iterative fitting procedure which makes use of four observables (^{1}H-^{1}H cross relaxation, ^{15}N longitudinal relaxation, multiexponential decay of the $2N_zH_z$ spin order and multiexponentional buildup of $2N_zH_z$ spin order) (Wang et al., 2000). The methods introduced in this paper rely on the second category. Here, we propose to follow separately the relaxation of each component of a ^{15}N doublet (the one, denoted N^α, corresponding to the α spin state of the bonded proton; the second, denoted N^β, corresponding to the other spin state). Previously, a related strategy was used for extracting ^{13}C chemical shift tensor in organic compounds (Walker et al., 2002) with detection at the heteronucleus level. In order to apply the method to proteins, the indirect detection of heteronuclei via protons is compelling. Moreover, it is noteworthy that such methods can suffer from signal overlap in coupled 2D spectra, particularly for ^{1}H-coupled ^{1}H-^{15}N HSQC spectra of proteins greater than 10 kDa. In fact, the problem of signal overlap can be partially solved using the IPAP scheme (Ottiger et al., 1998) as recently demonstrated (Hall et al., 2003): two separate ^{1}H-coupled ^{1}H-^{15}N HSQC spectra are recorded, one with the ^{15}N doublet in-phase (IP) and the other with this doublet in an anti-phase (AP) configuration. Consequently, the two spectra have to be added and subtracted in order to isolate each spin state but without the penalty of a somewhat arbitrary scaling which occurs in previous methods (Tjandra et al., 1996). The subsisting drawback of this procedure is that the signal overlap problem is only partially solved because ^{1}H-coupled spectra are involved. An alternative strategy was introduced by Marion and colleagues (Boisbouvier et al., 1999) and successfully applied to the measurement of carbon-13 transverse cross-correlation rates in nucleic acids. It consists of selecting and editing the $^{13}C^\alpha$ and $^{13}C^\beta$ states in two independent experiments. Taking up their strategy, we introduce novel pulse sequences adapted to the case of proteins and extended so as to measure the longitudinal ^{15}N csa/dipolar relaxation interference. We use a pulse sequence element S^{2}ED (Spin State Echo Differentiation, Bouguet-Bonnet et al., 2003) derived from the one proposed by Sorensen and colleagues (Meissner et al., 1997). The insertion of this filter in a classical ^{1}H-coupled ^{1}H-^{15}N HSQC spectrum allows us to select only one of the components of the ^{15}N doublet: N^α or N^β. Thus, when it is inserted in an inversion-recovery or Carr–Purcell–Meiboom–Gill relaxation measurement, we can follow separately the evolution of N^α and N^β, and therefore access to the interference term which corresponds to the difference in relaxation of these two components. It can be recalled that this procedure yields *only one* peak per residue in the 2D spectrum (for the N^α experiment *and* for the N^β experiment) and thus circumvents optimally the problem of overlaps which occurs in a ^{1}H coupled HSQC spectrum at the expense of a sensitivity loss by a factor two and, for extracting longitudinal cross-correlation rates, the need to include the classical nitrogen-15 auto-relaxation rates and the longitudinal two-spin order relaxation rates.

Longitudinal cross-correlation measurement

The full sequence is displayed in Figure 1a. The S^{2}ED filter (shaded pulses) is inserted in the inverse-detected inversion-recovery experiment (Farrow et al., 1994) after the first INEPT. The $\pi/2$ pulse at the end of the S^{2}ED inverts one of the ^{15}N doublet components while the other is defocused by the field gradient pulse applied at the beginning of the mixing time. The recovery of selected component is followed classically by varying the mixing time τ. Moreover, the phase cycles were set for obtaining a decay toward zero. The α/β selection is achieved by modifying the π pulse phase of the S^{2}ED subsequence: $\psi_N = 5\pi/8$ (or $13\pi/8$) for N^α and $\psi_N = 3\pi/8$ (or $11\pi/8$) for N^β. Two sets of spectra are collected: one corresponding to the recovery of N^α and the other to N^β. Because the resulting spectra can be decoupled in both dimensions, quantitative analysis can be performed with the same integration pattern map irrespective of the selected spin state. This ensures an identical processing for the two data sets. Experimentally, the behavior of the representative decay curves obtained for each of the two nitrogen doublet components is not mono-exponential (Figure 2a). In order to explain this phenomenon, we must describe completely the spin system evolution taking into account several quantities: N_z (nitrogen-15 magnetization), H_z^N (magnetization of the proton which is directly bonded to ^{15}N) and H_z^o (magnetization of other protons in the immediate surroundings of ^{15}N). Therefore the relevant basis of operators is:

$$\{N_z, H_z^N, H_z^o, 2N_zH_z^N, 2N_zH_z^o, 2H_z^NH_z^o, 4N_zH_z^NH_z^o\}$$

As suggested by Wang et al. (Wang et al., 2000), spin diffusion may occur as follows: $N_z \rightarrow 4N_zH_z^NH_z^o \rightarrow 2N_zH_z^o \rightarrow 2N_zH_z^N$. However, according to our simulations (Figure 3), the effect of

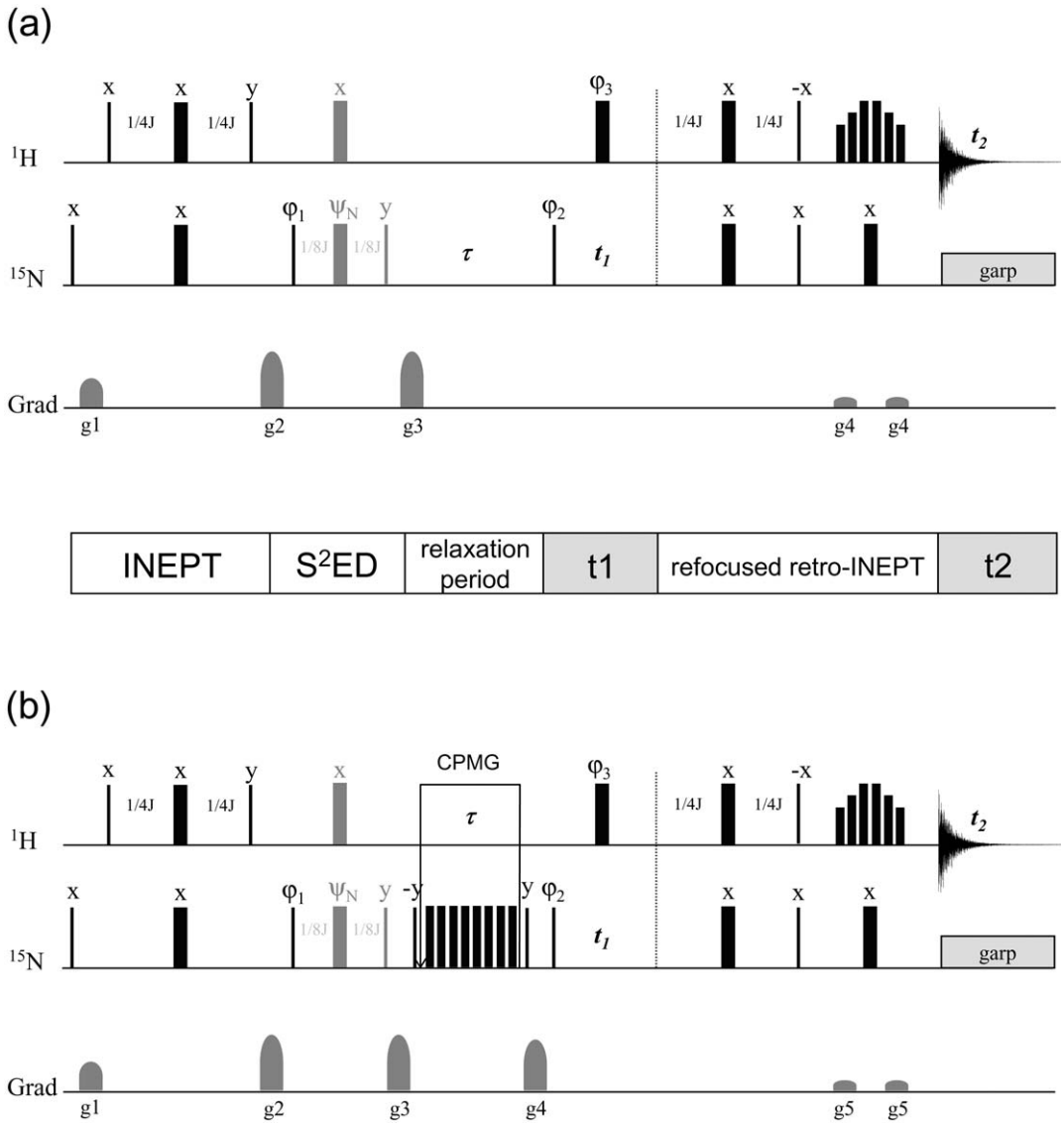

Figure 1. Pulse sequences for ^{15}N-^{1}H dipolar/^{15}N csa cross-correlation measurement. Narrow (wide) bars represent $\pi/2$ (π) flip angle pulses. Quadrature detection in the indirect dimension is achieved by incrementing $\varphi 2$ in States-TPPI fashion (Marion et al., 1989). J is set to the average ^{15}N-^{1}H scalar coupling constant (91 Hz). ^{15}N decoupling during ^{1}H detection is achieved using GARP (Shaka et al., 1985). Water signal was suppressed with 3-9-19 watergate technique (Sklenár et al., 1993). (a) Longitudinal cross-correlation measurements. Gradient strengths $g_{1,2,3,4}$ = (800 us, 40.0 G/cm), (800 us, −40.0 G/cm), (1.6 ms, −13.0 G/cm), (800 us, 10.0 G/cm). Complete phase cycling: φ_1 = x, −x; φ_2 = y; φ_3 = x, x, −x, −x; ψ_N = 4 (13π/8), 4 (5π/8) or ψ_N = 4 (11π/8), 4 (3π/8) for selection of N^{α} or N^{β}, respectively; receiver = x, −x, x, −x. (b) Transverse cross-correlation. Gradient strengths $g_{1,2,3,4,5}$ = (800 us, 40.0 G/cm), (800 us, −40.0 G/cm), (1.6 ms, −13.0 G/cm), (1.6 ms, −26.0 G/cm), (800 us, 10.0 G/cm). Complete phase cycling: φ_1 = x, −x; φ_2 = y; φ_3 = x, x, −x, −x; ψ_N = 4 (13π/8), 4 (5π/8) or ψ_N = 4 (11π/8), 4 (3π/8) for selection of N^{α} or N^{β}, respectively; receiver = x, −x, x, −x.

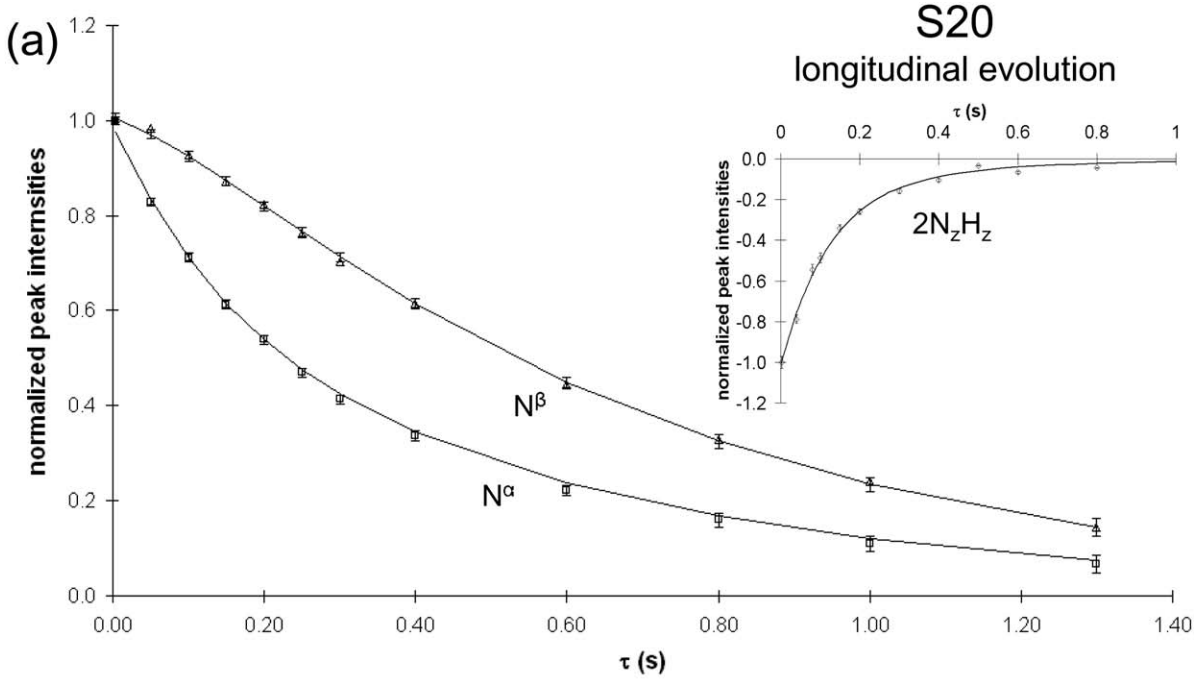

Figure 2. Representative decay curves for peak intensities obtained with the GIFA package (Pons et al. 1996). Data are displayed for residue S20 of ^{15}N-ubiquitin (a) Longitudinal cross-correlation measurements using the pulse sequences of Figure 1a at 14.1T. Diamonds and squares indicate the N^{α} and N^{β} behaviours, respectively. Data corresponding to the measurement of the two-spin longitudinal order relaxation rate are displayed in the inset (relaxation rate: $R_1^{2N_zH_z} = 6.55\ \mathrm{s}^{-1}$). Continuous curves represent the best fit of the three data sets (see text). (b) Transverse cross-correlation measurements using the pulse sequences of Figure 1b at 14.1T. Diamonds and squares indicate the N^{α} and N^{β} behaviours respectively. Continuous curves represent the best fit; each curve has been adjusted separately.

Complete system

N_z	H_z^N	H_z^O	$2N_zH_z^N$	$2N_zH_z^O$	$2H_z^NH_z^O$	$4N_zH_z^NH_z^O$
3.141	0.113	0.000	1.633	-0.014	0.000	-0.025
	0.347	-0.139	-0.025	0.000	-0.003	0.004
		0.151	0.000	-0.001	0.006	0.000
			3.201	-0.164	0.004	-0.017
				2.652	0.000	1.639
					2.093	-0.025
						3.064

Reduced system

N_z	$2N_zH_z^N$
3.141	1.633
	3.201

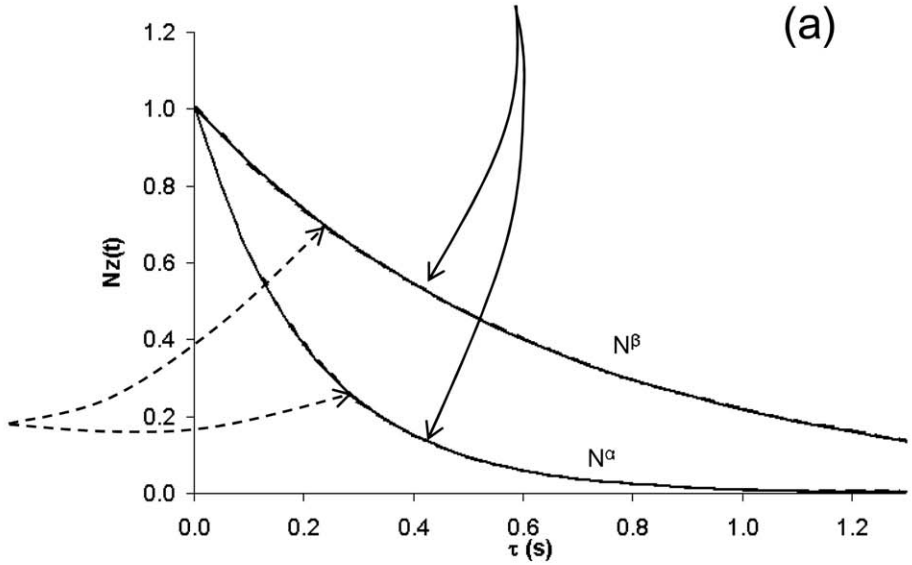

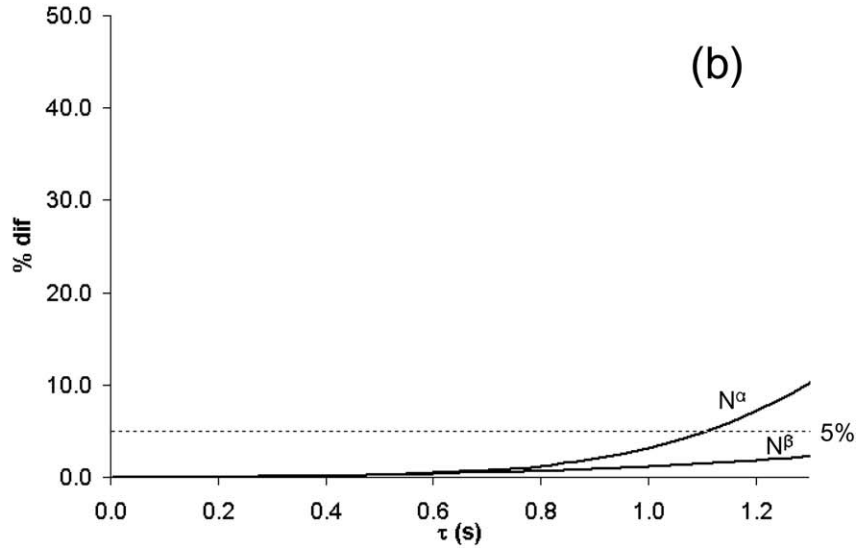

Figure 3. (a) Simulations of the magnetization decay resulting from the sequences of Figure 1a performed with relaxation rates calculated at $B_0 = 9.4$T, with $\tau_c = 4.5$ ns, $\tau_f = 30$ ps and $S^2 = 0.85$ (corresponding to a Lipari-Szabo model), $\Delta\sigma_N = -170$ ppm (csa of amide nitrogen ^{15}N, assumed to be axially symmetric), $\Delta\sigma_H = -10$ ppm (csa of amide proton ^{1}H, assumed to be axially symmetric), $r_{NH^N} = 1.02$ Å, $r_{NH^o} = 3.3$ Å and $r_{H^NH^o} = 3.4$ Å (corresponding to the averages of distances in NMR structure of ubiquitin from 1d3z.pdb). The analytical expressions of relaxation rates that have been used are those given in the paper of Wang et al., 2000. Solid lines are for full spin space (with the corresponding relaxation matrix top of figure) while dashed lines are for the reduced spin space with its associated relaxation matrix on the left. Initial conditions: $Nz(0) = \pm\frac{\gamma_H}{\gamma_N}\frac{Neq}{2}$ and $2NzHz(0) = \pm\frac{\gamma_H}{\gamma_N}\frac{Neq}{2}$ (for N^α) or $\mp\frac{\gamma_H}{\gamma_N}\frac{Neq}{2}$ (for N^β). (b) Difference (%) obtained when using both systems. Small (negligible) differences appear only at relatively long mixing times (2% at 1 s).

spin diffusion and of cross-relaxation proved to be negligible when using the pulse sequences of Figure 1a. In fact, the resolution of the set of differential equations governing the evolution of the above quantities requires the knowledge of the initial conditions at the beginning of the mixing time. The first ^{15}N $\pi/2$ pulse followed by a gradient pulse destroys nitrogen magnetization; therefore, neither longitudinal order $\gamma_N(2N_zH_z)$ nor nitrogen polarization $\gamma_N(N_z)$ exists at the beginning of the mixing time and we are thus only dealing with polarization transferred from proton. As only one nitrogen branch is inverted (hence the 1/2 factor in the expressions below) according to the ^{15}N π pulse phase in S^{2}ED and considering the two step phase cycle (φ_1), the initial conditions ($\tau = 0$s) for the two relevant quantities are:

$$N_z(0) = \pm\frac{\gamma_H}{\gamma_N}\frac{Neq}{2}, \tag{1}$$

$$\begin{aligned} 2N_zH_z(0) &= \pm\frac{\gamma_H}{\gamma_N}\frac{Neq}{2} \quad (\text{for } N^\alpha) \\ \text{or} \quad &\mp\frac{\gamma_H}{\gamma_N}\frac{Neq}{2} \quad (\text{for } N^\beta). \end{aligned} \tag{2}$$

Using these initial conditions, the simulations provided the undisputed evidence that spin diffusion is negligible up to relatively long mixing times (Figure 3). In comparison, the initial conditions are totally different if we follow directly the buildup of the longitudinal two-spin order from N_z, as it is the case for the experiments of Wang et al. (Wang et al., 2000) or Kover et al. (Kover and Batta, 2001):

$$N_z(0) = -\frac{\gamma_H}{\gamma_N}Neq, \tag{3}$$

$$2N_zH_z(0) = 0. \tag{4}$$

For these initial conditions, spin diffusion may occur and cannot be neglected as apparent in our computer simulations (see Figure 4), this feature being in perfect agreement with the conclusions of Wang et al. (2000). The fact that our approach does not suffer from spin diffusion comes actually from other initial conditions (see Equations 1 and 2). Consequently, considering the pulse sequences of Figure 1a, the spin space can safely reduce to the subspace $\{N_z, 2N_zH_z^N\}$ with two evolution equations derived from the extended Solomon equations:

$$\frac{dN_z(t)}{dt} = -R_1^N(N_z(t) - N_{eq}) - \eta_z(2N_zH_z(t)) \tag{5}$$

$$\frac{d2N_zH_z(t)}{dt} = -R_1^{2N_zH_z}(2N_zH_z(t)) - \eta_z(N_z(t) - N_{eq}),$$

where R_1^N is the nitrogen longitudinal relaxation rate, η_z the ^{15}N csa/dipolar cross-correlation rate and $R_1^{2N_zH_z}$ the two-spin order longitudinal relaxation rate. N_{eq} stands for the thermal equilibrium nitrogen magnetization.

Because of the necessity to fit non exponential curves corresponding to eqs. (5), the measurements of R_1^N and $R_1^{2N_zH_z}$ are mandatory. Actually R_1^N could be treated as an adjustable parameter but we found that it is useless to refine it further (data not shown, no significant change on the results). Consequently, three data sets were used simultaneously in the fitting procedure: one corresponding to the N^α experiments, the second to the N^β experiments and the third to the measurement of the longitudinal two-spin order relaxation rate $R_1^{2N_zH_z}$. In the longitudinal two-spin order experiment, data were obtained without a π pulse during the mixing time, that is without suppressing the effects of cross-correlation. More precisely, eqs. (5) were used to adjust η_z and $R_1^{2N_zH_z}$. For N^α experiments, initial conditions are $N_z(0) = +\frac{\gamma_H}{\gamma_N}\frac{Neq}{2}$ and $2N_zH_z(0) = +\frac{Neq}{2}$, N_z being the observable; for N^β experiments, initial conditions are $N_z(0) = +\frac{\gamma_H}{\gamma_N}\frac{Neq}{2}$ and $2N_zHz(0) = -\frac{\gamma_H}{\gamma_N}\frac{Neq}{2}$, N_z being the observable; and for $2N_zHz$ experiments, initial conditions are $N_z(0) = -\frac{\gamma_H}{\gamma_N}\frac{Neq}{2}$ and $2N_zH_z(0) = -\frac{\gamma_H}{\gamma_N}\frac{Neq}{2}$, $2N_zH_z$ being the observable. An excellent agreement between recalculated and experimental data is obtained (Figure 2a), and this, even at long mixing times as predicted by the simulations. It is obvious that the fact that non exponential decays are observed constitute a drawback of the method in the case of longitudinal cross-correlation measurements. The requirement of two additional experiments (for R_1^N and $R^{2N_zH_z}$) is not really a penalty because these measurements must anyway be performed in a study aiming at characterizing the dynamics of a protein. Moreover, the simultaneous fitting of η_z and $R_1^{2N_zH_z}$ experiments ensures that cross-correlation effects are properly taken into account in the $R_1^{2N_zH_z}$ measurement. From the experimental point of view, a minimum of eight mixing times is recommended in order to describe correctly the whole decay curves. Typically, the range of mixing times must cover a signal decay of 80%, and therefore include long mixing times.

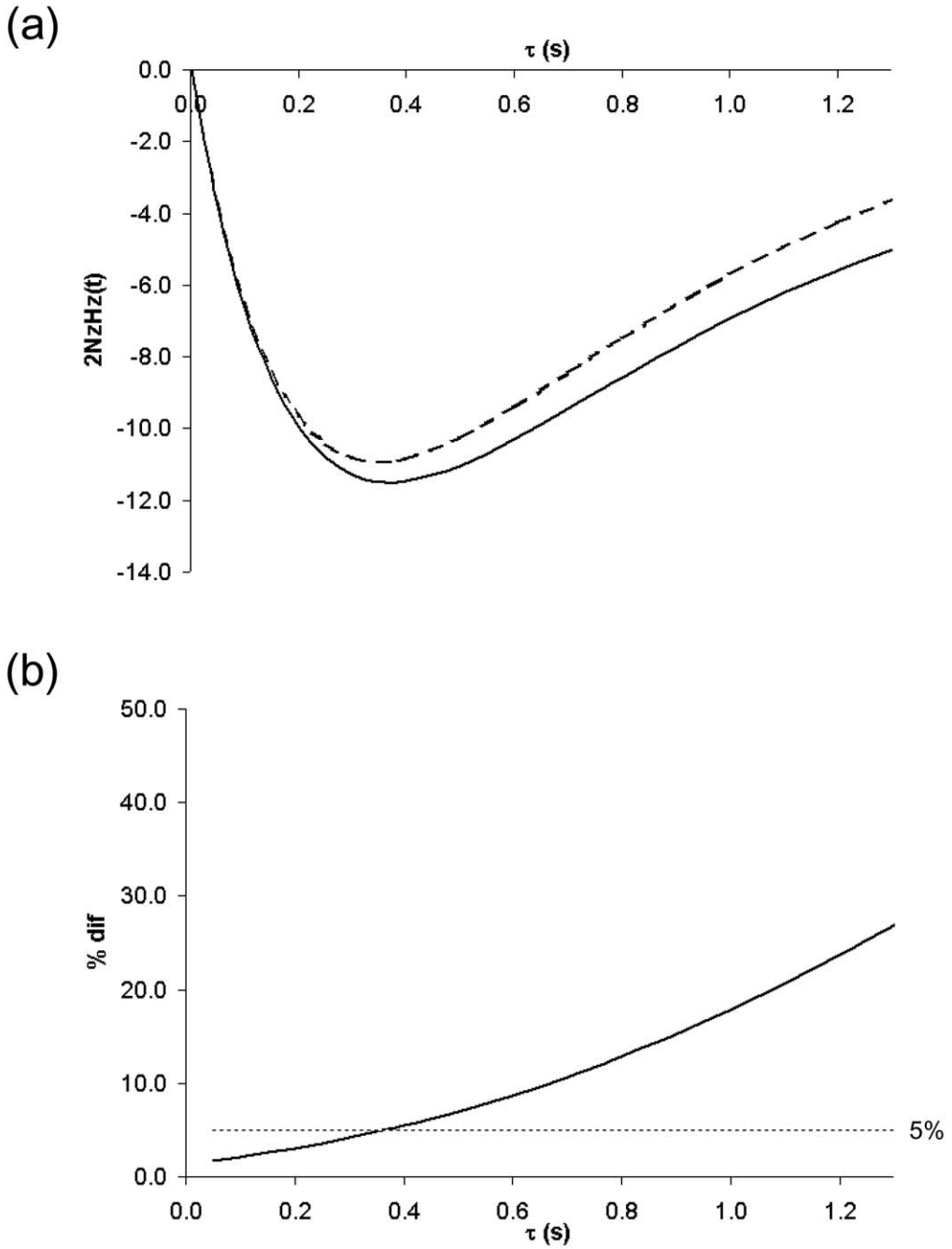

Figure 4. (a) Simulations of the magnetization decay resulting from the inversion of the nitrogen magnetization with the aim of probing the creation of the longitudinal two-spin order magnetization. Simulations have been performed with the same relaxation rates as those in Figure 3. Initial conditions: $Nz(0) = -\frac{\gamma_H}{\gamma_N} Neq$ and $2NzHz(0) = 0$. (b) Difference (%) obtained when using both systems.

Transverse cross-correlation measurement

The sequence (Figure 1b) starts exactly in the same way as before in order to eliminate nitrogen magnetization at the beginning of the mixing time. The S^2ED filter is inserted prior to the classical Carr-Purcell-Meiboom-Gill experiment after the first INEPT. As for longitudinal measurements, α/β selection is achieved by modifying the π pulse phase in the S^2ED subsequence: $\psi_N = 5\pi/8$ (or $13\pi/8$) for N^α and $\psi_N = 3\pi/8$ (or $11\pi/8$) for N^β. The next $\pi/2$ pulse stores one of the ^{15}N doublet components along the z-axis while the other is defocused by a field gradient pulse. Thereafter the stored component is taken back to the xy-plane and its decay is followed by incrementing the number of loops in the CPMG pulse train. During the evolution period, no ^1H pulse is applied so as to avoid any mixture of (α) and (β) spin states. After the nitrogen chemical shift labeling (t_1), the ^{15}N polarization is converted into observable proton magnetization. As in the previous sequence, decoupling is applied in both dimensions.

As described previously (Goldman, 1984; Boisbouvier et al., 1999), the spin dynamics in the transverse plane is governed by:

$$\frac{d}{dt}\begin{pmatrix} N_+ \\ 2N_+H_z \end{pmatrix} = -R\begin{pmatrix} N_+ \\ 2N_+H_z \end{pmatrix} \text{ with}$$

$$R = \begin{pmatrix} R_2^N & \frac{\eta_{x,y}}{2} + i\pi J_{NH} \\ \frac{\eta_{x,y}}{2} + i\pi J_{NH} & R_2^{NH} \end{pmatrix}. \quad (6)$$

R_2^N and $R^{NH}2$ being the transverse relaxation rates of N_+ and $2N_+H_z$, respectively, $\eta_{x,y}$ the csa-dipolar transverse cross-correlation rate, and J_{NH} the scalar one-bond coupling constant. This can be transformed in the basis of the operators $N_+^\alpha = \frac{1}{2}(N_+ + 2N_+H_z)$ and $N_+^\beta = \frac{1}{2}(N_+ - 2N_+H_z)$:

$$\frac{d}{dt}\begin{pmatrix} N_+^\alpha \\ N_+^\beta \end{pmatrix} = -R'\begin{pmatrix} N_+^\alpha \\ N_+^\beta \end{pmatrix} \text{ with } R' =$$

$$\begin{pmatrix} \overline{R_2} + \frac{\eta_{x,y}}{2} - i\pi J_{NH} & \Delta R_2 \\ \Delta R_2 & \overline{R_2} - \frac{\eta_{x,y}}{2} + i\pi J_{NH} \end{pmatrix} \quad (7)$$

with $\overline{R_2} = \frac{1}{2}(R_2^N + R_2^{NH})$ and $\Delta R_2 = \frac{1}{2}(R_2^N - R_2^{NH})$. This latter quantity can be omitted in the above matrix because, here, the difference between the diagonal elements, $(\eta_{x,y} + 2i\pi J_{NH})$, is much bigger than ΔR_2 (Goldman, 1984). $\overline{R_2}$ is the transverse relaxation rate averaged over the nitrogen in-phase and anti-phase components. To make effective such an averaging, the values of mixing times delays have to be chosen as multiples of $1/4J_{NH}$. In this way, the apparent relaxation rate constants R_2^α and R_2^β are obtained from the mono-exponential intensity decay of well-resolved cross-peaks in a series of 2D experiments. Figure 2b shows the typical decay of the two components associated with the residue S20 of ubiquitin. It must be pointed out that, because the two experiments are independent, neither particular spectra processing nor combination of data between the two spectra is required, as it is the case for many other methods (Tjandra et al., 1996; Tessari et al., 1997; Hall et al., 2003; Pelupessy et al., 2003). The extraction of apparent relaxation rates from the decay curves is identical to the one usually performed for obtaining transverse auto relaxation rates. The corresponding interference term η_{xy} is obtained by the difference of these apparent relaxation rates:

$$\left.\begin{aligned} R_2^\alpha &= \overline{R_2} + \frac{\eta_{xy}}{2} \\ R_2^\beta &= \overline{R_2} - \frac{\eta_{xy}}{2} \end{aligned}\right\} \eta_{xy} = R_2^\alpha - R_2^\beta\,. \quad (8)$$

The two experimental curves can also be fitted simultaneously as previously reported (Hall et al., 2003) and one can, if necessary, use only short mixing time values so as to minimize possible multi-spin relaxation effects. In our case, as it can be observed in Figure 2b, both decays are mono-exponential and we can exclude any multi-spin effect.

Results

The validity of all experiments is demonstrated on a ^{15}N labeled ubiquitin sample (1.4 mM in H_20 95%: D_2O 5%, pH = 4.7, Na acetate buffer, VLI Research) at 300K. Measurements were made at 9.395T and 14.093T on Bruker Avance DRX spectrometers (^1H resonance frequency: 400 MHz and 600 MHz, respectively). Spectra were acquired with spectral widths of 8.4 kHz and 1.8 kHz in the ^1H and ^{15}N dimensions, respectively. For the measurement of longitudinal cross-correlation rates, the experimental parameters were as follows; number of scans: 32 (400 MHz) and 16 (600 MHz), recycling delay: 4 s, 128 t_1 increments. α state and β state experiments were interleaved for several values of the mixing time (2, 50, 100, 150, 200, 250, 300, 400, 600, 800, 1000, and 1300 ms). For the measurement of transverse cross-correlation rates,

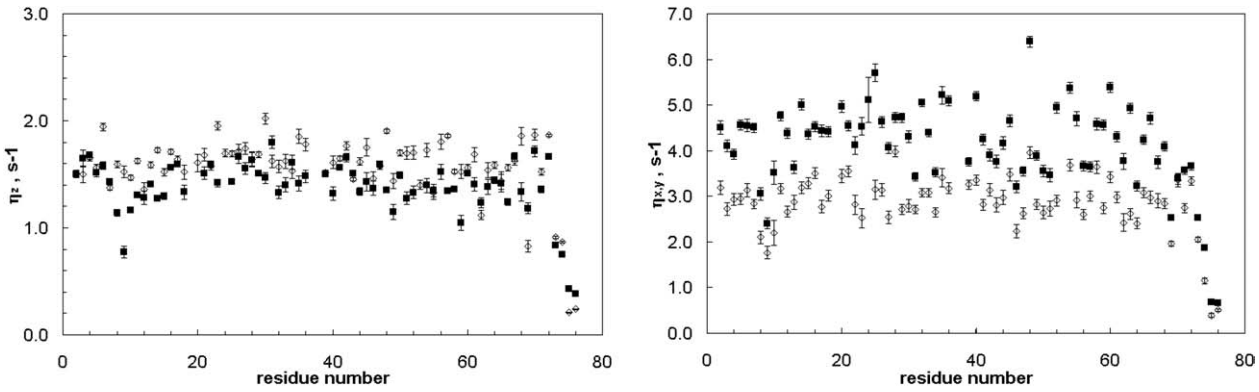

Figure 5. ^{15}N relaxation data measured for ubiquitin. Left: longitudinal cross-correlation rates η_z obtained with the pulse sequences of Figure 1a at 9.4T (open diamonds) and at 14.1T (filled squares). Right: transverse cross-correlation rates $\eta_{x,y}$ obtained with the pulse sequences of Figure 1b at 9.4T (open diamonds) and at 14.1T (filled squares).

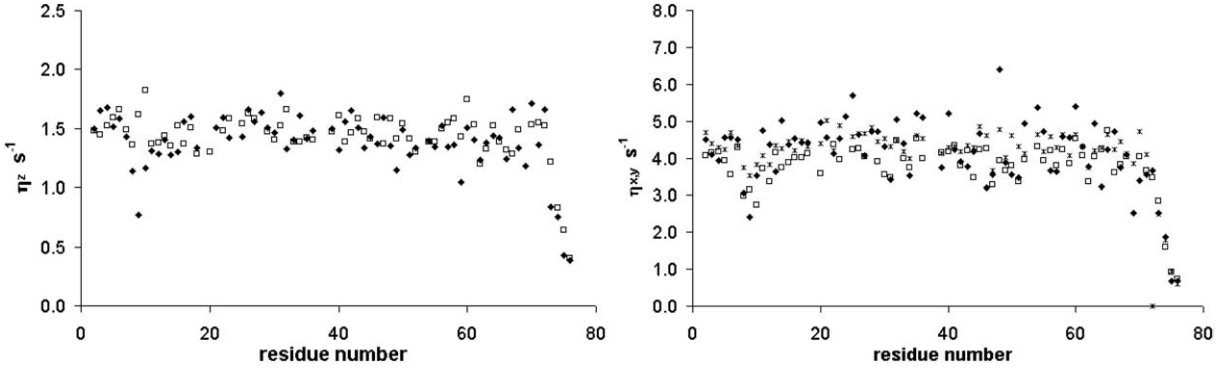

Figure 6. Comparison between the η values obtained at 14.1T for ubiquitin: data obtained with the pulse sequences of Figure 1a (left) or 1b (right) at 14.1T (filled diamonds), data published by Tjandra et al. (1996) (stars), and data published by Kover et al. (2001) (open squares). Left: longitudinal cross-correlation rates η_z, right: transverse cross-correlation rates $\eta_{x,y}$. It is noteworthy that, in the article of Tjandra et al., $\eta_{x,y}$ are not directly available, the corresponding values have been recalculated with the material provided in their article.

the experimental parameters were as follows; number of scans: 32 (400 MHz) and 16 (600 MHz), recycling delay: 4 s, 128 t_1 increments. The CPMG pulse train was calibrated at a power level such as $|\gamma B_1|/2\pi = 16.6$ kHz (this corresponds to $\pi/2$ pulse duration of 60 μs) and an echo delay of 880 μs. The relaxation decays were sampled at eight times: 16, 48, 80, 112, 144, 192, 256, and 320 ms. Data processing was carried out with the GIFA version 4.4 program (Pons et al., 1996). The GIFA extension for relaxation was used to deduce the apparent transverse relaxation rates (R_2^α and R_2^β) from peak intensities. A homemade program was written for fitting the longitudinal cross-correlation rates according to the extended Solomon equations. The outputs are displayed on Figure 5 for the backbone amides of human ubiquitin. The η_{xy} and η_z values determined here are compared (Figure 6) with those presented at 14.1 T for ubiquitin (η_z, Tjandra et al., 1996; η_{xy} and η_z, Kover et al., 2001). For η_z a reasonable agreement is found whereas, for η_{xy}, the three sets of results are much more scattered. Nevertheless, and as expected, the η_{xy} scale linearly with R_2 values (η_z with R_1, respectively) in agreement with the theoretical prediction (Fushman and Cowburn, 1998). Moreover, an average factor of 1.5, corresponding to the ratio of magnetic field values, is found between η_{xy} at 14.1T and η_{xy} at 9.4T as expected as far as a predominant contribution of the spectral density at zero frequency is assumed.

Discussion and conclusion

Most of the methods designed to measure the ^{15}N csa/dipolar relaxation interference require two separate experiments, their comparison leading to the desired cross-correlation rates. As it was made clear

by recent articles (Hall et al., 2003; Pelupessy et al., 2003), the success of the measurement depends of several factors. On the one hand, the two sequences should be nearly identical to avoid any scaling factor between the two experiments; on the other hand the signal overlap problem must be addressed. The two sets of pulse sequences presented in this article fulfill efficiently these requirements with, however, the penalty of a sensitivity loss. Concerning pulses and delays, the two sequences are identical; only one pulse phase has to be modified from one experiment to the other, thus avoiding the recourse to any scaling factor in their processing. Moreover, because the direct observation of a single spin state is achieved within each experiment, the combination (addition or subtraction) of two HSQC spectra is not required as with the IPAP scheme (Ottiger et al., 1998). Finally, no signal overlap problem is encountered as the spectra do not contain the superposition of in-phase and anti-phase components. It can be admitted that the proposed method, as far as longitudinal cross-correlation measurements are concerned, is not straightforward; it requires additional relaxation parameters and a more complex analysis of experimental data. Although this latter point could be considered as a drawback, the additional effort is not considerable and this affords the possibility of measuring in identical conditions longitudinal cross-correlation rates and longitudinal spin-order auto-relaxation rates. In conclusion, we have introduced a novel experimental approach to measure both ^{15}N csa/dipolar longitudinal and transverse cross-correlation terms by means of spin state selective measurements. This strategy could be extended to the measurement of any relaxation parameter that acts differently on the two spin states.

Acknowledgements

We are most grateful to the 'Service Commun de Biophysicochimie des Interactions Moléculaires', directed by the Prof. G. Branlant (University of Nancy I), for the use of their 14.1 T Bruker Avance spectrometer. Prof. C. Roumestand (University of Montpellier II) is thanked for helpful discussions and its advices concerning the setup of the experiments.

References

Boisbouvier, J., Brutscher, B., Simorre, J.P. and Marion, D. (1999) *J. Biomol. NMR.*, **14**, 241–252.

Bouguet-Bonnet S., Mutzenhardt P. and Canet D. (2003) *Magn. Reson. Chem.*, **41**, 1030–1033.

Brutscher, B. (2000) *Concepts Magn. Reson.*, **12**, 207–229.

Farrow, N.A., Muhandiram, R., Singer, A.U., Pascal, S.M., Kay, C.M., Gisn, G., Shoelson, S.E., Pawson, T., Forman-Kay, J.D. and Kay, L.E. (1994) *Biochemistry*, **33**, 5984–6003.

Ferrage, F., Eykin, T.R. and Bodenhausen, G. (2004) *ChemPhysChem*, **5**, 76–84.

Fuschman, D. and Cowburn, D. (1998) *J. Am. Chem. Soc.*, **120**, 7109–7110.

Fuschman, D., Tjandra, N. and Cowburn, D. (1998) *J. Am. Chem. Soc.*, **120**, 10947–10952.

Ghose, R., Huang, K. and Prestegard, J.H. (1998) *J. Magn. Reson.*, **135**, 487–499.

Goldman, M. (1984) *J. Magn. Reson.*, **60**, 437–452.

Hall, J.B. and Fushman, D. (2003b) *Magn. Reson. Chem.*, **41**, 837–842.

Hall, J.B., Dayie, K.T. and Fushman, D. (2003a) *J. Biomol. NMR.*, **26**, 181–186.

Kover, K.E. and Batta, G. (2001) *J. Magn. Reson.*, **150**, 137–146.

Kroenke, C.D., Loria, J.P., Lee, L.K., Rance, M. and Palmer III, A.G. (1998) *J. Am. Chem. Soc.*, **120**, 7905–7915.

Kumar, A., Grace, R.C.R. and Madhu, P.K. (2000) *Prog. NMR Spectrosc.*, **37**, 191–319.

Marion, D., Ikura, M., Tschudin R. and Bax, A. (1989) *J. Magn. Reson.*, **85**, 393–399.

Meissner, A., Duus, J.O. and Sorensen, O.W. (1997) *J. Magn. Reson.*, **128**, 92–97.

Ottiger, M., Delaglio, F. and Bax, A. (1998) *J. Magn. Reson.*, **131**, 373–378.

Pelupessy, P., Espallargas, G.M. and Bodenhausen, G. (2003) *J. Magn. Reson.*, **161**, 258–264.

Pervushin, K., Riek, R., Wider, G. and Wüthrich, K. (1997) *Proc. Natl. Acad. Sci. USA*, **94**, 12366–12371.

Pons, J.L., Malliavin, T.E. and Delsuc, M.A. (1996) *J. Biomol. NMR*, **8**, 445–452.

Scheurer, C., Skrynnikov, N.R., Lienin, S.F., Straus, S.K., Bruschweiler, R. and Ernst, R.R. (1999) *J. Am. Chem. Soc.*, **121**, 4242–4251.

Shaka, A.J., Freeman, R. and Barker, P.B. (1985) *J. Magn. Reson.*, **64**, 547–552.

Sklenár, V., Piotto, M., Leppik, R. and Saudek, V. (1993) *J. Magn. Reson. Ser. A*, **102**, 241–245.

Tessari, M., Vis, H., Boelens, R., Kaptein, R. and Vuister, G.W. (1997) *J. Am. Chem. Soc.*, **119**, 8985–8990.

Tjandra, N., Szabo, A. and Bax, A. (1996) *J. Am. Chem. Soc.*, **118**, 6986–6991.

Walker, O., Mutzenhardt, P., Tekely, P. and Canet, D. (2002) *J. Am. Chem. Soc.*, **124**, 865–873.

Wang, L., Kurochkin, A.V. and Zuiderweg, E.R.P. (2000) *J. Magn. Reson.*, **144**, 175–185.